Int J Adv Manuf Technol (2017) 93:1–9
DOI 10.1007/s00170-015-7391-9

ORIGINAL ARTICLE

A study to estimate the tensile strength of friction stir welded AA 5059 aluminium alloy joints

N. Babu[1] · **N. Karunakaran**[1] · **V. Balasubramanian**[2]

Received: 22 February 2015 / Accepted: 3 June 2015 / Published online: 23 June 2015
© Springer-Verlag London 2015

Abstract Friction stir welding (FSW) is an important welding technique where in, and optimizing the process parameters will improve the joint strength of the welds. The FSW process and tool parameters play a major role in determining the joint strength. In this paper, an attempt has been made to establish an empirical relationship between the FSW process parameters (rotational speed, welding speed, and axial force) and predicting the maximum tensile strength of the joint. Statistical tools such as design of experiments, analysis of variance, and regression analysis are used to develop the relationships. A non-heat treatable aluminum alloy Aluminium Association 5059 of 4 mm thickness was used as the base material. Response surface methodology is employed to develop the mathematical model. Analysis of variance technique is used to check the adequacy of the developed mathematical model. The developed mathematical model can be used effectively at 95 % confidence level. The effect of FSW process parameter on mechanical property of Aluminium Association 5059 aluminum alloy has also been analyzed in detail.

Keywords Aluminium alloy · Anova · Friction stir welding · Response surface methodology

✉ N. Babu
babu.manu11@gmail.com

[1] Department of Mechanical Engineering, Annamalai University, Annamalai Nagar 608002, Tamil Nadu, India

[2] Department of Manufacturing Engineering, Annamalai University, Annamalai Nagar 608002, Tamil Nadu, India

1 Introduction

Friction stir welding (FSW), patented by The Welding Institute in 1991, is a newer technique for material joining and processing. FSW has enjoyed worldwide interest because of its advantages over traditional joining techniques [1]. This technology boasts reduction of distortion and elimination of cracking due to the solid-state joining, low distortion in long welds, excellent mechanical properties in the weld and heat-affected zone, no fumes or spatters, low shrinkage, as well as being energy efficient, when compared to conventional fusion welds. The weld zone from FSW has a fine worked or recrystallized grain structure, generated by stirring and forging of the parent alloy [2, 3]. To date, the application fields of FSW are marine (hulls and superstructures), aerospace (fuselages, wings, and fuel tanks), railway (high speed trains and carriages), automotive (chassis, wheel rims, space frames, and truck bodies), motorcycle, electrical, and refrigeration industries. Lakshminarayanan and Balasubramanian [4] optimized the FSW parameters of RDE-40 aluminum alloy using the Taguchi technique. In this study, the Taguchi approach was applied to determine the most influential factors that yielded better tensile strength of friction stir welded RDE-40 aluminum alloy joints. The results indicated that rotational speed, welding speed, and axial force are the significant parameters in deciding the tensile strength of the welded joint. Blignault et al. [5] optimized the procedures for FSW of 5083-H321 aluminum alloy by selecting appropriate weld process parameters and tool modifications. The model developed in this study allows the weld tensile strength to be predicted for all combinations of tool geometry and process parameters [6–8]. Raja kumar et al. [9] optimized FSW process to attain maximum tensile strength of AA7075-T6 aluminum alloy by using the central composite face-centered (CCF) design of experiment (DOE). In their study, an attempt was made to establish

an empirical relationship between the FSW process parameters, tool dimension, hardness, and the tensile strength of the joint. Statistical tools such as DOE, Analysis Of Variance (ANOVA), and regression analysis were used to develop the relationships. The response surface methodology (RSM) [10] was used to analyze the effects of process parameters. Elongovan et al. [11] reported the effect of FSW process parameters on mechanical properties of FS welded AA 6061 aluminum alloy. They found that the tensile strength initially increased with the increase in tool rotational speed, welding speed, and axial force, but the tensile strength decreased after reaching a maximum value. Studies on the micro structure and mechanical properties of friction stir welded AA 5083 aluminum alloy showed that the decrease in friction heat flow results in the refinement of grain size, higher ductility, and better formability [12]. Aluminium alloy AA 5059 is a newly developed armor grade aluminum alloy which is mainly recommended in the ship hull and super structure due to its beneficial properties like high corrosion resistance, high strength to weight ratio, formability, etc. [13]. The effects of FSW process parameters on the mechanical properties of aluminum alloy AA 5059 have not been analyzed, hence, an attempt has been made to develop a mathematical model to predict the tensile strength of friction stir welded AA 5059 aluminum alloy. The developed models are tested for their adequacy and accuracy using ANOVA and confirmation tests, respectively. From literature, it is understood that rotational speed, welding speed, and axial force influence the heat generation and flow of the plasticized material and eventually affect the micro structure and mechanical properties of the weld. The ANOVA was employed to investigate the influence of input parameters, tool rotational speed, and welding speed on tensile property of the weld. Hence, the objective of this work was to develop RSM by creating empirical relationships relating the FSW input parameters and output response.

2 Experimental work

The material used in this investigation is AA 5059. The chemical composition and mechanical properties of the base material are presented in Tables 1 and 2, respectively. The rolled plates of 4 mm thickness were machined to the required size (150×75 mm), and the welding was carried out in butt joint configuration using FSW machine which developed by R.V.S. machine tool, Coimbatore as shown in Fig. 1. The details regarding tool dimension used in this investigation to fabricate the joints are presented in Table 3. To fabricate the joints a non consumable tool which was made of high speed steel was used. Tool tilt angle 2.5° was maintained in this work. The photograph of the fabricated joint is displayed in Fig. 2. The tool having the ratio of shoulder diameter to pin diameter (D/d) as 3 has been chosen for this study because it is having good joining properties among various pin configurations [14]. Tensile specimens were prepared as per the American Society for Testing of Materials (ASTM E8M-04) standards [15] to evaluate the tensile properties of the joints. Tensile test was carried out on an electro-mechanically controlled universal testing machine at 100 kN (FIE, India; UNITECH 94001). The specimens extracted from the mid section of the welded plates were used for the tensile, hardness and micro structural analysis is shown in Fig. 3. The yield strength, ultimate tensile strength, elongation, and joint efficiency were recorded from tensile specimen. The samples for observations were prepared by standard metallographic procedures and etched with Keller's reagent (2 mL HF, 3 mL Hcl, 5 mL HNO_3, and 190 mL water) to reveal the grain structure of the welded joints. Micro structural analysis was carried using a light optical microscope (MEIJI), Japan model; ML7100 with an image analyzing software. Vickers's micro hardness testing machine (Shimadzu, Japan) was employed to measure the hardness across the joint under 0.50 N load. The tensile-tested specimens were examined in a Scanning Electron Microscope (Make- JEOL India Ltd; Model–JSM −6610 LU) to observe the fractured surface morphology Fig. 4 shows the tensile specimens before and after testing.

Table 1 Chemical composition of base material AA 5059

Si	Fe	Cu	Mn	Mg	Zn	Ti	Al
0.041	0.1	0.003	0.933	5.21	0.001	0.489	Remaining

Table 2 Mechanical properties of base material AA 5059

Yield strength (MPa)	Tensile strength (MPa)	Elongation in 50 mm gauge length (%)	Micro hardness $HV_{0.5}$
350	385	16	123

Fig. 1 Photograph showing experimental setup of FSW machine

Table 3 Details regarding FSW tool

Profile	Pin length (mm)	Tool shoulder diameter (mm)	Pin diameter (mm)	Tool tilt angle (deg)
Taper threaded	3.7	12	4	2.5

3 Results

3.1 Response surface methodology

RSM [14] is an interaction of mathematical and statistical techniques for modeling and optimizing the response variable models where several independent variables influence a dependent variable or response. The goal is to optimize the response [15]. Experiments have been carried out according to the experimental plan based on central composite rotatable second-order design (CCD) matrix with the star points being at the center of each face of factorial space. The upper limit of a factor was coded as +1, and the lower limit was coded as −1. The "face-centered CCD" involves 20 experimental observations for three independent input variables. The experimental FSW parameters and their levels in this study in the actual form are given in Table 4.

3.2 Identifying the important process parameter

A large number of trial runs were carried out using 4-mm-thick rolled plates of AA 5059 aluminum alloy to find out the feasible working limits of FSW process parameters. The working range of each process parameter was decided upon by inspecting the macro structure for smooth appearance without any visible defects such as tunnel defect, pinhole, kissing bond, etc. When the rotational speed was lower than 600 rpm, wormhole at the retreating side of weld nugget was observed and it may be due to insufficient heat generation and insufficient metal transportation; on the other hand, when the rotational speed was higher than 1300 rpm, tunnel defect was observed and it may be due to excess turbulence caused by higher rotational speed. Similarly, when the welding speed was lower than 10 mm/min, pinhole type of defect was observed due to excess heat input per unit length of weld and vertical movement of the metal; when the welding speed was higher than 40 mm/min, tunnel defect at the bottom in the retreating was observed due to inadequate flow of material caused by insufficient heat input. When the axial force was lower than 2.8 kN, tunnel defect and crack like defect at the middle of the weld cross section in retreating side were observed due to the absence of vertical flow of material caused by insufficient downward force; when the axial force was increased beyond 4.0 kN, it resulted in large mass of flash and excessive thinning due to higher heat input.

3.3 Development of design matrix

The selected design matrix is a three factor five level central composite rotatable designs consisting of 20 sets of coded conditions composed of a full factorial $2^3=8$, plus 6 center points and 6 star points thus 20 experimental runs allowed the estimation of the linear, quadratic, and two way interactive effects of the process parameter on the mechanical properties.

3.4 Recording the response

Transverse tensile properties of friction stir welded AA 5059 aluminum alloy joints were evaluated by using universal testing machine. The average values of the results obtained from those specimens are tabulated and presented in Table 5.

3.5 Developing the mathematical model

The adequacy of the developed empirical relationship for the response variable tensile strength was tested using the

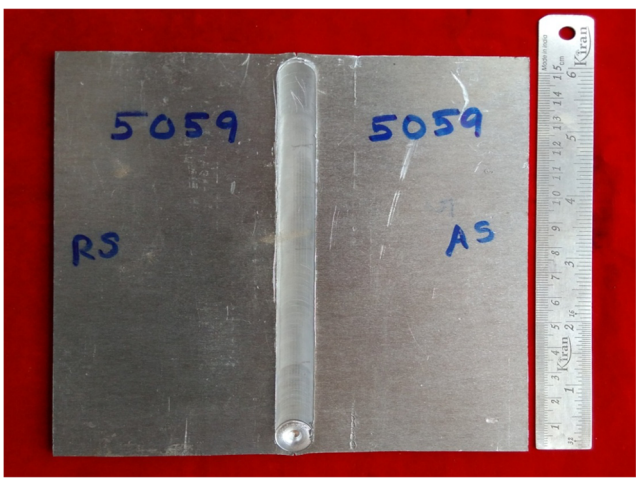

Fig. 2 Photograph of the fabricated FSW joint

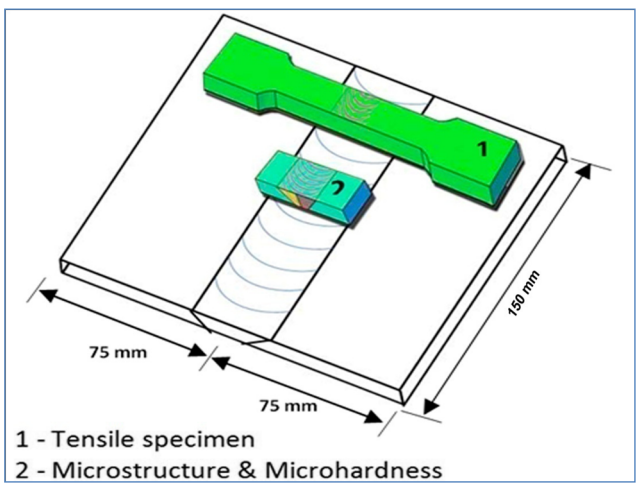

Fig. 3 Scheme of extraction of specimens from welded joints

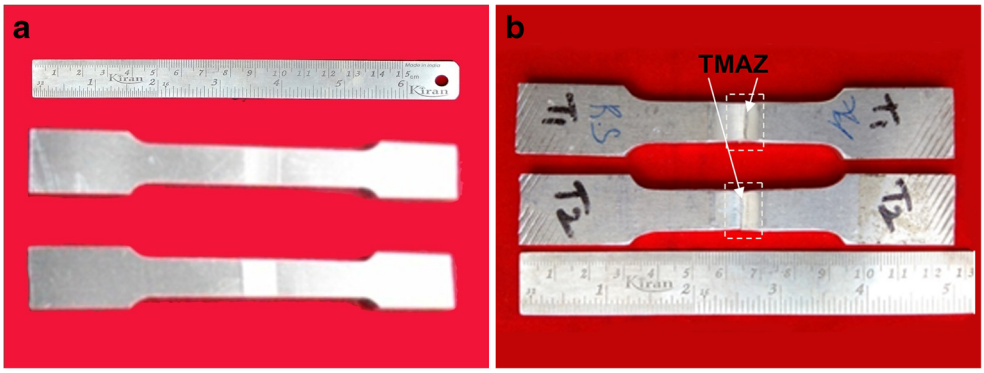

Fig. 4 **a** Photograph of tensile specimens (before fracture). **b** Photograph of tensile specimens (after fracture)

ANOVA technique [16]. The fit summary reveals that the fitted quadratic model is statistically significant to analyze the response variables. It is found that the calculated F ratios are larger than that of the tabulated values at a 95 % confidence level; hence, the models are considered to be adequate. Another criterion that is commonly used to illustrate the adequacy of a fitted regression model is the coefficient of determination (R^2), which compares the range of the predicted value at the design point to the average prediction error. In order to estimate the regression coefficient, a number of experimental design techniques are available. In this work, CCF design was used which fits the second-order response surface accurately. This requires three levels of each factor. The factors are rotational speed, welding speed, and axial force that are expressed as

$$Y = f(N, S, F) \quad (1)$$

where

Y The response (ultimate tensile strength)
N Rotational speed, rpm
S Welding speed (mm/min)
F Axial force (kN).

For three factors, the selected polynomial (regression) could be expressed as

$$Y = b_0 + b_1N + b_2S + b_3F + b_{11}N^2 + b_{22}S^2 + b_{33}F^2 + b_{12}NS + b_{13}NF + b_{23}S \quad (2)$$

All the coefficients were obtained applying CCF design using the design expert statistical software package. After determining the significant coefficients (at 95 % confidence level), the final model was developed using only these coefficients and the developed final mathematical model to estimate tensile strength is given below:

$$\text{Tensile strength (TS)} = \{293.32 + 7.70(N) - 6.00(S) - 2.82(F) + 2.00(NS) - -2.75(NF) - 2.25(SF) - 7.79(N^2) - 12.91(S^2) - 8.31(F^2)\}\ \text{MPa} \quad (3)$$

3.6 Checking the adequacy of the developed model

The adequacy of the developed model was tested using the ANOVA technique, and the results of the second-order response surface model fitting in the form of ANOVA are given in Table 6. The determination of coefficient (R^2) indicates the goodness of fit for the model. The value of adjusted determination coefficient (adjusted R^2=0.9968) is also high, which indicates a high significance of the model. Predicted R^2 is also made a good agreement with the adjusted R^2. All the above consideration indicates an excellent adequacy of the regression model.

4 Discussion

To obtain the influencing tendency of process and the effects of the different process parameters on tensile strength, the three-dimensional diagrams are plotted under certain processing conditions. Equation (3) is plotted in Fig. 5 as surface plots for each of the process parameter. It is clear from these figures that the tensile strength varies with the increase of process parameters such as rotational speed, welding speed, and axial force. The apex of response plot gives the maximum tensile strength. These response contours can help in the prediction of the tensile strength at any zone of the experimental domain. A contour plot is produced to visually display the region of optimal factor

Table 4 Important process parameters and their level

Parameters	Units	Notation	−1.682	−1	0	1	1.682
Rotational speed	Rpm	N	600	741.9	950	1158	1300
Welding speed	mm/min	S	10	16.1	25	33.1	40
Axial force	kN	F	2.8	3.0	3.4	3.8	4.0

Table 5 Machining design matrix and measured response

No	FSW process parameters			Properties	% of error
	Rotational speed (rpm)	Welding speed (mm/min)	Axial force (kN)	Tensile strength (MPa)	
1	−1	−1	−1	263	8.99
2	1	−1	−1	279	3.46
3	−1	1	−1	259	10.38
4	1	1	−1	275	4.84
5	−1	−1	1	268	7.26
6	1	−1	1	273	5.53
7	−1	1	1	247	14.53
8	1	1	1	260	10.03
9	−1.682	0	0	257	11.07
10	1.682	0	0	285	1.38
11	0	−1.682	0	266	7.95
12	0	1.682	0	247	14.53
13	0	0	−1.682	275	4.84
14	0	0	1.682	264	8.65
15	0	0	0	293	1.38
16	0	0	0	294	1.73
17	0	0	0	293	1.38
18	0	0	0	294	1.73
19	0	0	0	292	1.03
20	0	0	0	294	1.73

settings. Predicted optimum tensile strength obtained from the response surface model is by using a rotational speed of 950 rpm, welding speed of 25 mm/min, and axial force of 3.4 kN. Perturbation plot shown in Fig. 6 illustrates the direct effect of the FSW parameters on the tensile strength for an optimized design. It is seen that as the rotational speed increases the tensile strength of FS welded aluminum alloy AA5059 increases and then it decreases. The highest rotational speed produces high heat generation, subsequently heat supplied to the base material is high, which causes turbulent material flow and grain coarsening in stir zone there by the tensile strength is lower. Neither low heat input nor high heat input is preferred in FSW. It is clear that in FSW as the rotational speed increases the heat input also increases. More heat input destroys the regular

Table 6 ANOVA results for tensile strength

Source	Sum of squares	df	Mean square	F Value	*p* value Prob>F	
Model	5171.84	9	574.648	514.96	<0.0001	Significant
A-N:Rotational speed	808.67	1	808.67	724.68	<0.0001	
B-S:Welding Speed	491.80	1	491.80	440.72	<0.0001	
C-N:Axial force	108.53	1	108.53	97.26	<0.0001	
AB	32.00	1	32.00	0.0003		
AC	60.50	1	60.50	54.22	<0.0001	
BC	40.50	1	40.50	36.29	0.0001	
A^2	874.10	1	874.10	<0.0001		
B^2	2403.6	1	2403.6	<0.0001		
C^2	997.20	1	997.20	<0.0001		
Residual	11.16	10	11.16			
Lack of fit	7.83	5	7.83	2.35	0.1853	Not significant
Pure error	3.33	5	0.019			
Cor total	5183	19				

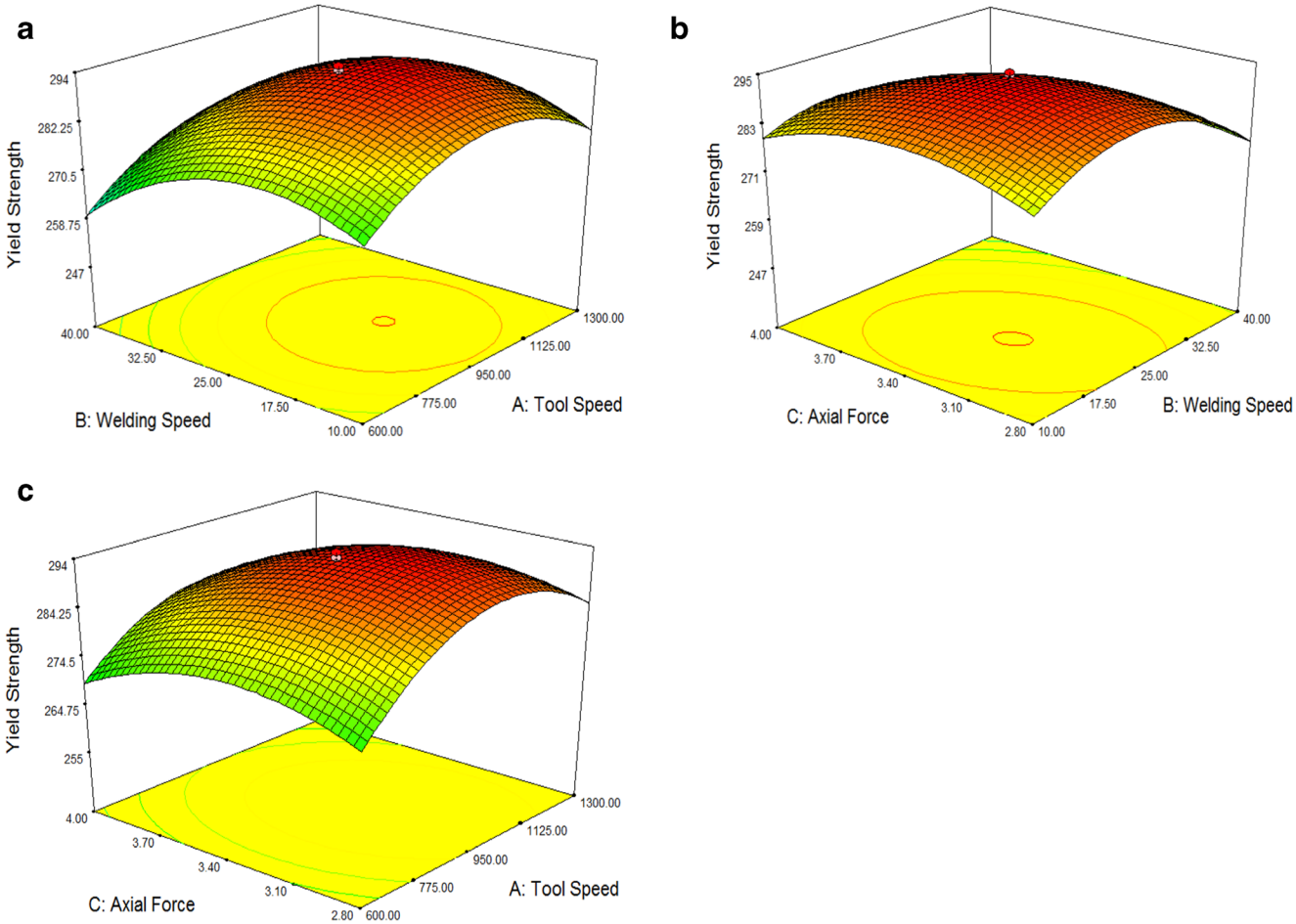

Fig. 5 **a** Response graphs for tensile strength. **b** Response graphs for tensile strength. **c** Response graphs for tensile strength

flow behavior. These results agree with Elangovan et al. [14]. When welding speed increases, the mechanical properties of the FSW aluminum alloy AA5059 increases and then decreases. At lowest welding speed (10 mm/min) and highest welding speed (40 mm/min), lower tensile strength is observed. This is due to the increased frictional heat and insufficient frictional heat

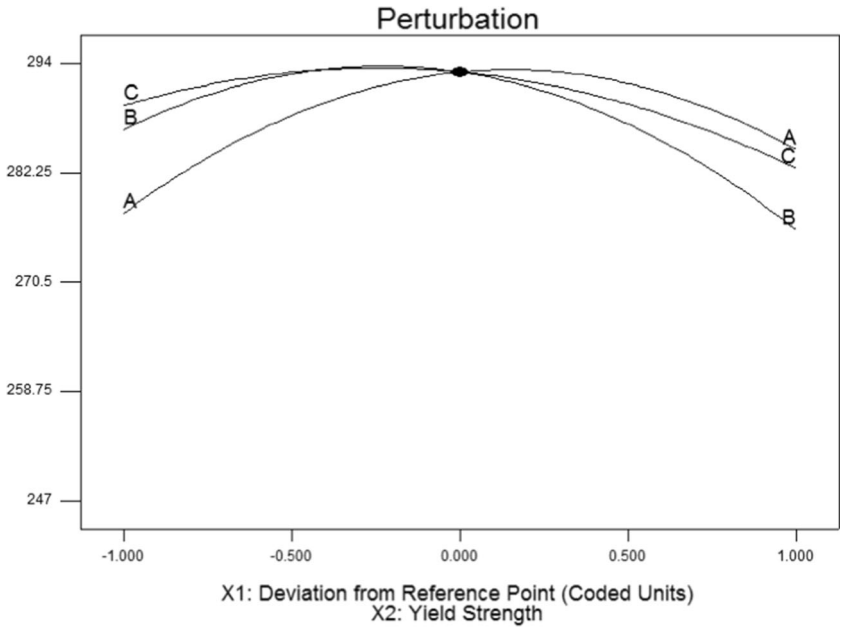

Fig. 6 Perturbation plot showing the effect of all factors on the tensile strength

generated, respectively [17]. Also, higher welding speed produces poor plastic flow of the material due to poor consolidation of the metal interface. When the axial force increases from 2.8 to 4 kN, the tensile strength of the weld material slightly increases and then decreases. This may be due to insufficient coalescence of transferred material. At highest axial force, the plunge depth of the tool into the work pieces is higher which results in lower tensile strength [18]. When rotational speed is compared with the welding speed, rotational speed is marginally more sensitive to changes in tensile strength.

4.1 Tensile properties

The tensile strength of base material was 385 MPa. The maximum tensile strength obtained in FSW welded joint was 294 MPa. Liu et al. [19] conducted tensile test to study the variation of strength property of 5083-H116 aluminum alloy due to the influence of FSW process parameters. It is proposed by them that the tensile strength of the welded material was about 297.5–311.8 MPa, and the tensile strength of the parent material was about 323.5 MPa. It is found that, in FSW, the fracture location is between weld nugget and the TMAZ on the advancing side, which happens to be the weakest point of the specimen. In practice, the reason for the fracture near the interface between the weld nugget and the TMAZ is the remarkable difference in the internal structure between the weld nugget and TMAZ. The weld nugget is composed of fine equiaxed grains, and TMAZ is composed of coarse-bent recovered grains. Therefore, the interface between weld nugget and TMAZ becomes a weaker region, and the joint is fractured at this interface during the tensile testing.

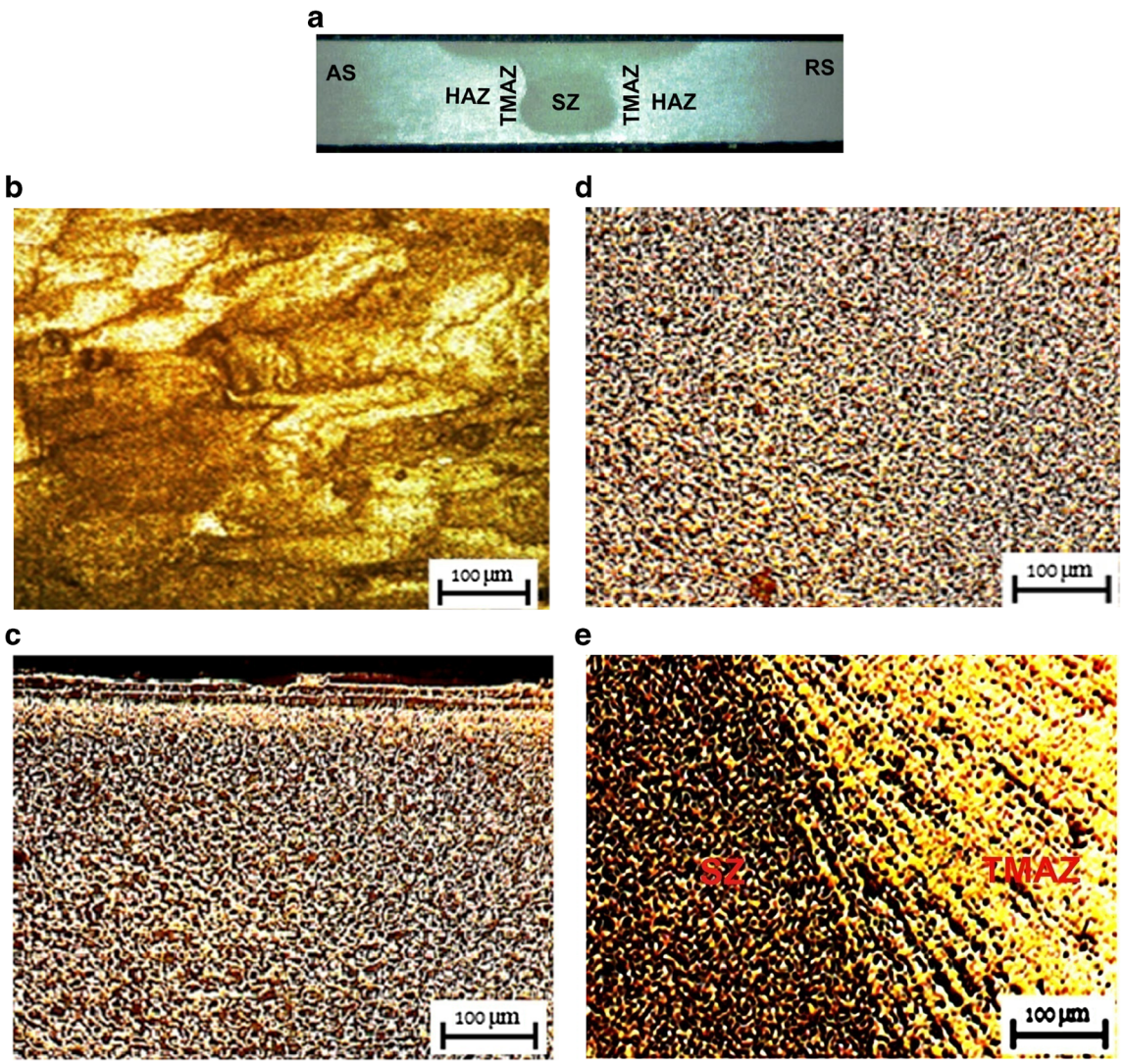

Fig. 7 **a** Macrograph of welded joint. **b** Micro structure of base material. **c** Shoulder influenced region (stir zone). **d** Pin influenced region (stir zone). **e** Interface between stir zone and TMAZ

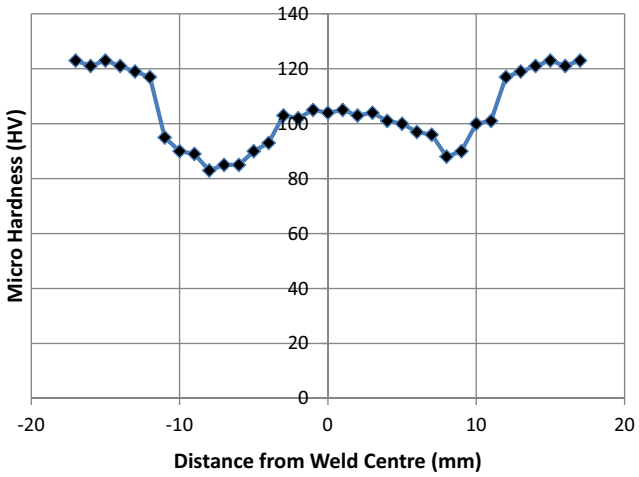

Fig. 8 Micro hardness distribution for FSW joints

4.2 Micro structure

The macro graph of FSW joint is shown in Fig. 7a. The micro structure of base material is shown in Fig. 7b. The matrix shows severely worked grains of primary phase and the particles of Mg-Al_2 and some insoluble Al_6 (Fe, Mn). The solubility of Mg in aluminum is lower, and hence, the particles of Mg-Al_2 are present and formed a banding along the direction of rolling. The particles in aluminium solid solution have fragmented and partially elongated with primary phase. Figure 7c shows the image of shoulder influenced zone in stir zone. The effect of constant stress with heat caused the evaporation of the Mg from the base metal. This has lead to the Mg depleted layer. The bottom of the shoulder layer is the nugget zone where the insoluble particles are uniformly fragmented due to stress and heat. No visible defects were observed. Figure 7d shows the nugget zone with fragmented particles of the constituents of AA 5059. Figure 7e is interface zone of parent metal which had undergone thermo mechanical transformation at the vicinity of the nugget zone. The orientation of the parent metal at the retreading side has changed. The left side shows the nugget zone and the right side is TMAZ zone. Because of fine grains, due to dynamic recrystallization, high hardness was recorded in this zone.

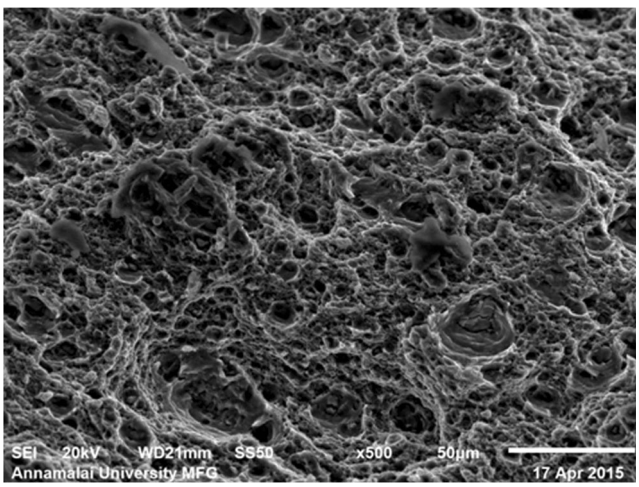

Fig. 9 SEM fractograph of tensile specimen

Table 7 Result of confirmation experiment

Process parameters			Tensile strength (MPa)		Error (%)
Rotational speed (N)	Welding speed (S)	Axial force(F)	Estimated (Mpa)	Experimentally predicted (Mpa)	
950	25	3.4	294	289	1.73

4.3 Hardness measurement

The base material in its initial condition showed hardness value of 123 Hv. The micro hardness distribution for the FSW joint is plotted in Fig. 8. FSW joint showed highest average micro hardness of 105 Hv at the weld zone, and this indicates that there was 15 % reduction in hardness at the weld zone. In FSW joint, lowest hardness is observed on the advancing side compared to retreating side. The hardness is lower than the base material due to dissolution of strengthening precipitates during the weld thermal cycle.

4.4 Fracture surface

The tensile specimen of welded joints of AA 5059 aluminum alloy was analyzed using SEM to reveal the fracture surface morphology. Fractured surfaces of the FSW welded sample after tensile test are shown in Fig. 9. Fine dimples are seen in fractured surface. Since fine dimples are a characteristic feature of ductile fracture, the FSW joints have shown higher ductility compared to all other joints, and this indicates a severe plastic deformation.

4.5 Model verification

Experiments are conducted to verify the regression equation. The optimized parameter was used to conduct an experiment, and the results were tabulated as shown in Table 7. The results were obtained and the error is 1.73 %.

5 Conclusions

1. The joint fabricated using a tool rotational speed of 950 RPM, welding speed of 25 mm/s, and an axial force of 3.4 kN exhibited superior tensile properties.
2. Empirical relationships were developed using statistical tool such as DOEs, regression analysis, and ANOVA to

predict the tensile strength of FSW joints at 95 % confidence level. The developed relationship is:

$$\text{Tensile strength (TS)} = \{293.32 + 7.70\,(\text{N}) - 6.00\,(\text{S}) - 2.82\,(\text{F}) + 2.00\,(\text{NS}) - 2.75\,(\text{NF}) - 2.25\,(\text{SF}) - 7.79\,(\text{N}^2) - 12.91(\text{S}^2) - 8.31(\text{F}^2)\}\ \text{MPa}$$

3. The interactive and individual effects of process parameters on responses are studied and found that rotational speed plays a dominant role to influences the tensile strength.
4. Confirmation experiments showed that the developed model is reasonably accurate.

Acknowledgments The authors are grateful to the CEMAJOR, Department of Manufacturing Engineering, Annamalai University, Annamalai Nagar, India for extending the facilities to carry out this investigation. The authors wish to place their sincere thanks to Mr. S. Karthikeyan, Research scholar, Annamalai University for his morale support.

References

1. Thomas W M, Nicholas E D, Needham J C, Dawes CJ (1991) Friction stir butt welding. International Patent Application No.PCT/GB9/02203.
2. Mishra RS (2005) Friction stir welding and processing. Mater Sci Eng 50:1–78
3. Nandan T, Bhadeshia KDH (2008) Recent advances in friction stir welding–process, weldment structure and properties. Prog Mater Sci 53:980–1023
4. Lakshminarayanan AK, Balasubramanian V (2008) Process parameters optimization for friction stir welding of RDE-40 aluminium alloy using Taguchi technique. Nonferrous Met Soc China 18:548–554
5. Blignault C, Hattingh DG, James MN (2012) Optimizing friction stir welding via statistical design of tool geometry and process parameters. J Mater Eng Perform 21(6):927–935
6. Karthikeyan R, Bala Subramanian V (2010) Prediction of the optimized friction stir spot welding process parameters for joining AA 2024 aluminum alloy using RSM. Int J Adv Manuf Technol 51(1–4):173–183
7. Zhang Z, Zhang HW (2007) Material behaviours and mechanical features in friction stir welding process. Int J Adv Manuf Technol 35:86–100
8. Bitondo C, Prisco U, Squillice A, Buonadonna P, Dionora G (2011) Friction stir welding of AA 2198 butt joints: mechanical characterization of the process and of the welds through DOE analysis. Int J Adv Manuf Technol 53:505–516
9. Raja kumar S, Muralidharan C, Balasubramanian V (2010) Establishing empricial relationships to predict grain size and tensile strength of friction stir welded AA 6061-T6 aluminium alloy joints. 1863–1872
10. Hamilton C, Dymek S, Blicharski M (2007) Mechanical properties of al 6061 welds by friction stir welding and metal inert gas welding. Arch Metall Mater 52:67–72
11. Elangovan K, Balasubramanian V, Babu S (2009) Predicting tensile strength of friction stir welded 6061 aluminium alloy joints by mathematical model. Mater Des 30:188–193
12. Liu Y, Wang W, Xie J, Sun S, Wang L, Qian Y, Meng Y, Wei Y (2012) Micro structure and mechanical properties of aluminium 5083 weldments by gas tungsten arc and gas metal arc welding. Mater Sci Eng A 549:7–13
13. Anderson T (2003) New developments within the Aluminium Shipbuilding Industry. 58:3–5
14. Elangovan K, Bala Subramanian V, Babu S, Balaswubramanian M (2008) Optimising friction stir welding parameters to maximize tensile strength of AA 6061 aluminium alloy joints. Int J Manuf Res 3:3
15. American society for testing and materials (ASTM). In Standard test methods for tension testing of metallic materials, vol. 03.01. West Conshohocken (PA): Annual book of ASTM standards.
16. Montogomery DC (1984) Design and analysis of experiments. Wiley, New York
17. Balasubramanian M, Jayabalan V, Balasubramanian V (2008) Developing mathematical models to predict tensile properties of pulsed current gas tungsten arc welded Ti-6Al-4V alloy. Mater Des 29:92–97
18. Rajakumar S, Muralidharan C, Balasubramanian V (2010) Optimization of the friction stir welding process and the tool parameters to attain a maximum tensile strength of AA7075-T6 aluminium alloy. J Eng Manuf 224:1175–1191
19. Hartawan A, Thoe T B, Ng, S T, Wu H, Liu K (2009) Initial Investigation of Friction Stir Welding. SIMTech Technical Reports: 10(1)